LIGHTWEIGHT STRUCTURES in CIVIL ENGINEERING
CONTEMPORARY PROBLEMS
Monograph from Scientific Seminar
Organized by Polish Chapters of
International Association for Shell and Spatial Structures
Lodz University of Technology
Faculty of Civil Engineering, Architecture and Environmental Engineering
XXIV LSCE
Łódź, 7th of December 2018 (Friday)

ANALYSIS OF LOCAL STABILITY OF DOUBLY CORRUGATED COLD-FORMED PROFILES

R. Walentyński [1] **R. Cybulski** [2]
[1] MSc PhD DSc, Associate Professor, Faculty of Civil Engineering, Silesian University of Technology, POLAND,
ryszard.walentynski@polsl.pl
[2] BSc MSc PhD, Assistant Professor, Faculty of Civil Engineering, Silesian University of Technology, POLAND,
robert.cybulski@polsl.pl

ABSTRACT: This paper describes the local stability analyses of doubly corrugated thin-walled (cold-formed) steel panels which are used as a solution for arch buildings and roofing structures. As an example of such system the ABM MIC 120 prefabrication technology is chosen where factory on wheels makes cold-formed arch steel buildings or roofs in a very short time period as self-supporting panels. The main problem of such structures lies in the lack of a proper theoretical model of the element due to its complex geometry. This leads to the significant overestimation of panel's ultimate load which in the worst case scenario, can cause a failure of a doubly corrugated structure. This work will shortly discuss the influence of surface transverse geometric imperfections called corrugations on the local stability of cold-formed elements. Authors of the paper compare results obtained from the analytical investigation, from linear and nonlinear numerical stability analyses and experimental investigation. The problem is more widely discussed in Ref. 8.

Keywords: cold-formed profiles, doubly corrugation, local stability, arch steel structures

1. INTRODUCTION

Due to today's difficult economy, cheap and short time consuming solutions for buildings industry are very desirable. One of the solutions which fulfills above requirements is the ABM (Automatic Building Machine) technology. It is a mobile factory used to fabricate and construct K-span arch steel buildings based on self-supporting panels made of MIC 120 and MIC 240 profiles. This technology comes from the USA and belongs to M.I.C. Industries Inc. Such a technology was commonly used by the US Army to build temporary buildings and nowadays these structures are becoming a popular solution in civilian life. The ABM technology consists of a movable, steel building manufacturing plant, known as the MIC 120 System. This machine is placed on a trailer, forming factory on wheels which can easily be transported to any construction sites (see Fig. 1).

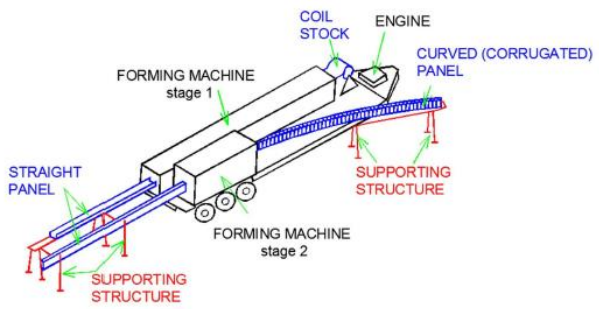

Fig. 1 The ABM prefabrication machine

Once, the machine is delivered to the site, the construction process can be started by a small group of trained crew. Firstly, a coil of steel is formed to a straight panel of channel cross-section. This panel is cut to achieve needed span of the future arch building and for some structures straight panels are used to build front walls (gable walls). Secondly, this panel is bent to form the arch and its shape changes due to surfaces' corrugations. Both shapes are shown in Fig. 2 where it can be observed that these panels consist of a main corrugation- obtained during the formation of a cross-section at stage 1, and a secondary corrugation-folded surfaces achieved from the panel's bend into an arch at stage 2. This is a reason for using the term a "doubly corrugated" steel arch panel. Such a terminology was also used by Mang in Ref. 1. The doubly corrugated panels are also called as corrugated panels or curved panels or crimped panel.

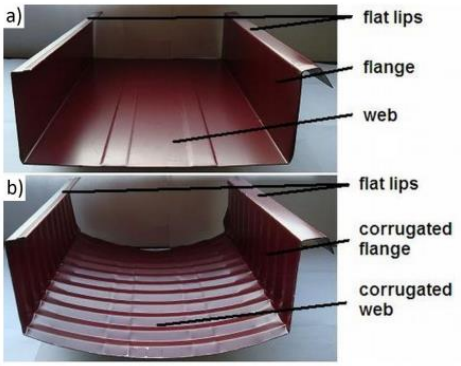

Fig. 2 Shapes of the ABM 120 panels: a) straight, b) doubly corrugated

After a few single panels are tightened together by the seam machine they are fixed to the lifting sling and transported to the execution place

by a crane. These groups of panels are seamed together to form an economical and waterproof steel structure.

The authors of this work have observed that in many projects, corrugations on panel's surfaces are neglected by engineers during calculation procedures. This leads to a significant overestimation of panel's ultimate load which in a worst case scenario can cause failures of a doubly corrugated structure. It must be stated that European design standards do not give a calculation procedure for elements with transverse imperfection such as corrugations. From the building's failure presented in Fig.3, it is observed that the key factor for understanding such collapses lies in the local behavior of neighboring single corrugations. A few days before this failure, some photos of this structure were taken, focusing on the top part of the arch. In Fig.4 it is clearly shown that instability which caused the collapse of the warehouse had a local character.

Fig. 3 The ABM building collapse (Poland)

Finally, the presented work can be useful for design purposes and can be treated as a warning for engineers who often thoughtlessly use design standards.

Fig. 4 Local instability before the collapse (Poland)

2. ANALYTICAL INVESTIGATION

The cross-section class of straight panels and curved panels is based on calculation given in Ref. 2. The calculation of critical load, effective width and post-critical load carrying capacity is based on Ref. 3. It must be clearly stated that given procedures do not take into account transverse geometrical imperfections such us corrugations. Young Modulus is equal to 203.3 GPa, Poisson ratio equals 0.3, yield strength f_y is equal 355.9 MPa, tensile strength equals 487.6 MPa and corresponding plastic strain 0.152. Thickness of metal sheet is equal 1 mm. Mechanical properties of metal sheet used for panel prefabrication are described in Ref. 4.

2.1. Straight panel

In Fig. 5 the effective cross-section area of a straight panel is presented.

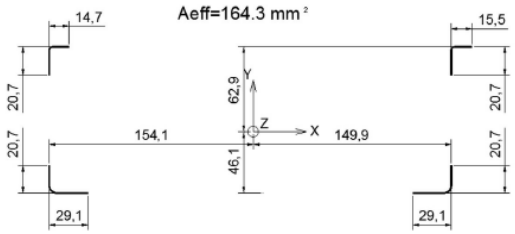

Fig. 5 Effective area of straight panel's cross-section

The post-critical load carrying capacity can be calculated as follows:

$$P_{u\_straight} = A_{eff} * f_y = 164.3 * 355.9 = 58.5 \text{ kN}. \quad (1)$$

2.2. Curved panel

In Fig. 6 the effective cross-section area of a straight panel is presented.

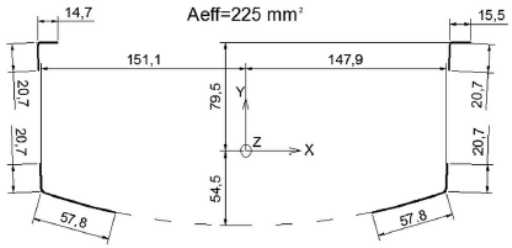

Fig. 6 Effective area of curved panel's cross-section

The post-critical load carrying capacity can be calculated as follows:

$$P_{u\_curvedt} = A_{eff} * f_y = 225 * 355.9 = 80.1 \text{ kN}. \quad (2)$$

3. NUMERICAL INVESTIGATION

Lengths of the panels samples are limited due to the hydraulic press clearance which is used in compression tests. So the effective length of each samples, which is measured between the clamps, is equal to 540 mm. This length is used in this research for numerical buckling investigation purposes.

3.1. Straight panel

The overall numerical model of straight panel made in ABAQUS software can be introduced where supports and load conditions are presented in Fig. 7. Plates and clamps from test setup are modeled as "rigid body" elements. Straight panel is modelled from "shell" elements with 26913 "quad-dominated" mesh elements of type S4R (a 4 node doubly curved shell with reduced integration, has six degrees of freedom at each node- three translations and three rotations).

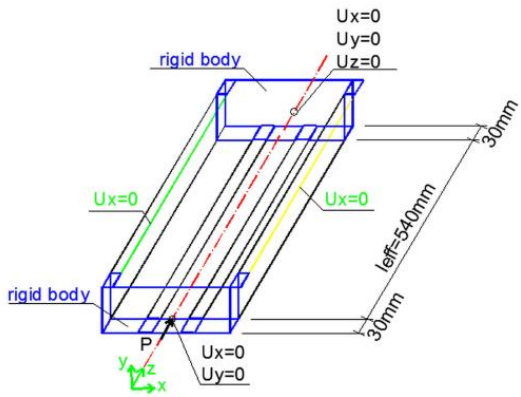

Fig. 7 Supports and load conditions for a straight panel

Three different types of analyses (conducted in ABAQUS FEM system) are used in order to investigate the post-buckling behavior of a straight panel: "Linear perturbation/ Buckle" (Ref. 5), "Riks Method" (Ref. 6), "Automatic Stabilization Method" (Ref. 7). The full description of different types of analyses is described in Ref. 8. In this paper brief description of only "Linear perturbation/ Buckle" and "Riks Method" is presented.

Firstly, linear buckling analysis is conducted in order to obtain critical buckling load at the bifurcation point (which lies somewhere on the equilibrium path). Such critical load is connected to the first eigenmode (deformation mode) and to the first eigenvalue. Unit concentrated load placed at the gravity centre of gross cross-section is applied. So the value of critical buckling load is equal to unit load times first eigenvalue (result in Newton "N"). That is why critical buckling load $P_{cr;B}$ = 17.74 kN. In this case first eigenmode corresponds to the situation where web deformes to a single half-wave towards inside of the cross-section. In the next step, obtained deformation field is exported to the Riks analysis based on arc length iteration method. Because for this nonlinear analysis concentrated load is applied at the effective gravity centre of the effective cross-section, which means that location of the concentrated load moved up. The deformation field scale factor is equal to 0.55 and it is with the minus sign (value is negative). So now the single half-wave is directed toward outside of cross-section-similar to the deformation obtained from laboratory tests. Such move helps to destroy straight element much faster than in case where deformation field would be taken straight from the linear buckling analysis. The value "0.55" stands for the U_Y displacement which is obtained from the classic nonlinear static analysis, where value of $P_{cr;B}$ was applied at the effective gravity centre. In such case where thickness of the wall is equal 1 mm, value of the imperfection is less important (as long as it is less than 1) and does not influence the final results. The sign of the imperfection value (positive or negative) is more important due to maximum failure load. From Riks analysis at the f_y compression stress level (355.9 MPa) the ultimate load P_U is equal to 61.12 kN. This value is similar to the value of ultimate load based on Eurocode calculations (Eqn. 1). The straight element collapse is observed at the compression stress level 369.9 MPa and this corresponds to failure force $P_{cr;M}$ = 63.77 MPa. Described analysis procedure is presented in Fig. 8. The load displacement path obtained from the Riks analysis is presented in Fig.9. It is observed that pre-buckling behavior is till $P_{cr;B}$ and post-buckling between $P_{cr;B}$ and $P_{cr;M}$. It can be stated the thin-walled elements with smooth walls (such as straight panel) have the post-buckling strength and do not collapse at the bifurcation point. In such case a secondary load path at a bifurcation point is considered as an ascendant branch of the load path.

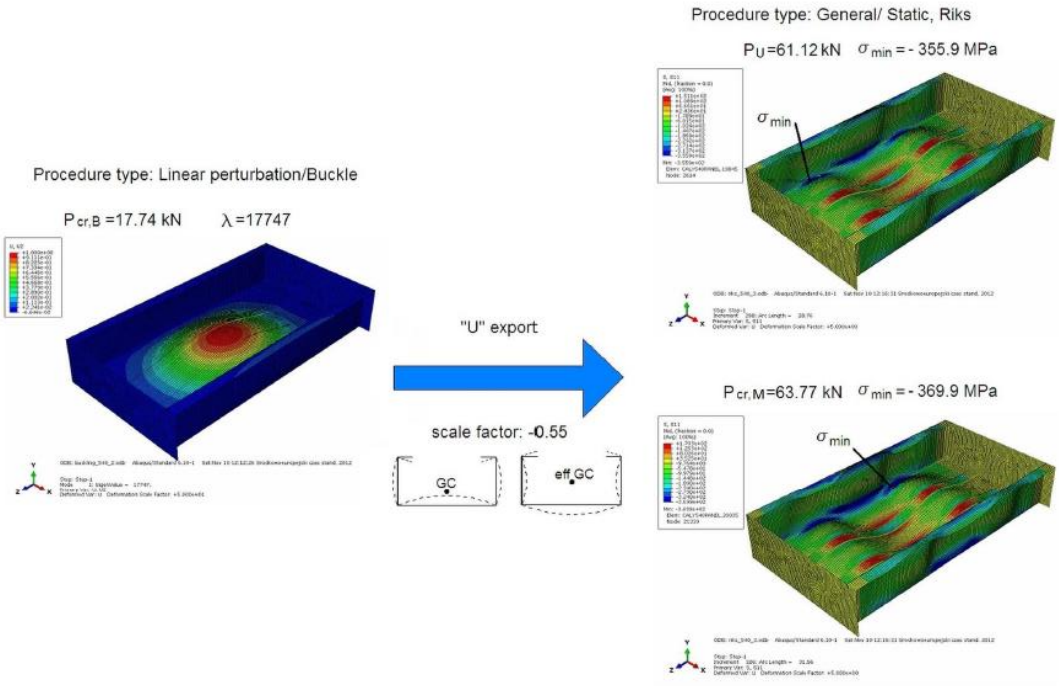

Fig. 8 Combined analysis: linear buckling and Riks method

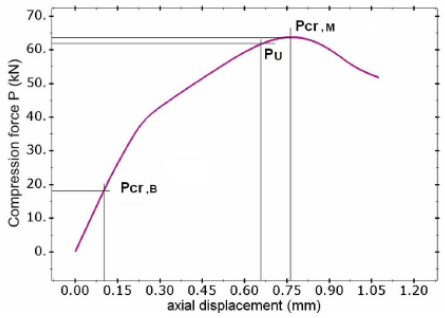

Fig. 9 Load-displacement path (linear buckling with Riks Method)

3.2. Doubly corrugated panel

The overall numerical model of curved panel can be introduced where supports and load conditions are presented in Fig. 10.

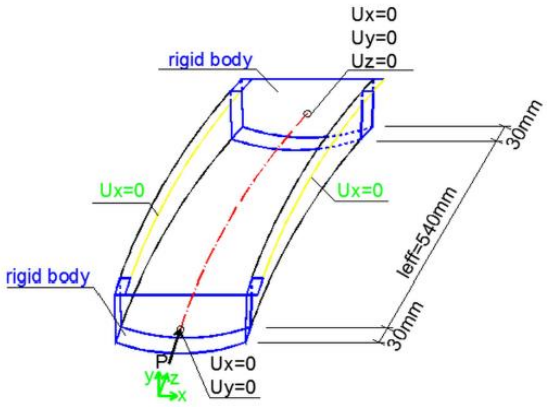

Fig. 10 Supports and load conditions for a curved panel

In this case, combined numerical methods (e.g. "Linear perturbation/ Buckle" and "Riks Method") are neglected due to the fact that geometrical imperfections are already on panel's surface and there is no need to add extra ones.
Models geometries were obtained from 3D optical scanning (Ref. 4, below Fig. 11).

Fig. 11 Set-up for 3D scanning

Each of the analyses were performed for panels samples cut out from arches with the following radiuses: 5 m, 7:5 m and 10 m.
For Linear Buckling analysis, concentrated load equal to 1 N was applied at the cross-section gravity centre. The first eigenmode obtained from this analysis is presented in Fig. 12.

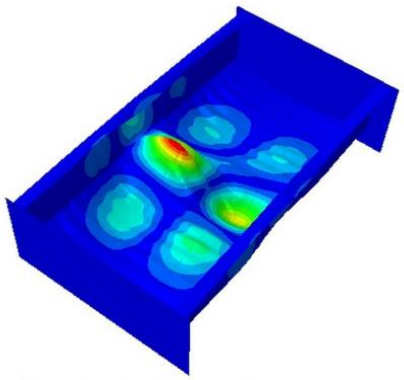

Fig. 12 Curved panel- first eigenmode

First eigenvalue is equal to $1.27 * 10^4$ and corresponds to critical buckling load with value 127 kN. This value is much larger than the post-critical load carrying capacity equal to 80.1 kN (Eqn. 2). It means that transverse geometrical imperfections have significant influence on the cold-formed buckling behaviour.
In order to run Riks analysis, the concentrated load equal to 30 kN was applied at the equivalent gravity centre of corrugated panel cross-section. Those analyses were done for the case where estimated total arc length is equal to 1 and arc length increments are following: initial 0.001, minimum $1 * 10^{-15}$, maximum 0.1. The position of the equivalent gravity centre was found by searching the location in which obtained failure load is the greatest one. Such assumption was necessary due to the low axial stiffness of surface corrugations. In Fig. 13 load paths for different arch radiuses are presented. From that it is observed that failure load has the smallest value for samples cut out from the arch of radius 5 m, middle value for sample from the arch of radius 7.5 m and the highest value for panel cut out from the arch of radius 10 m. The reason for that is as follows: for the biggest arch radius the corrugations are the smallest, so the failure load has the highest value; for the smallest arch radius the corrugations are the biggest, so the failure load has the lowest value. This phenomenon is caused by the prefabrication process of the curved panels.

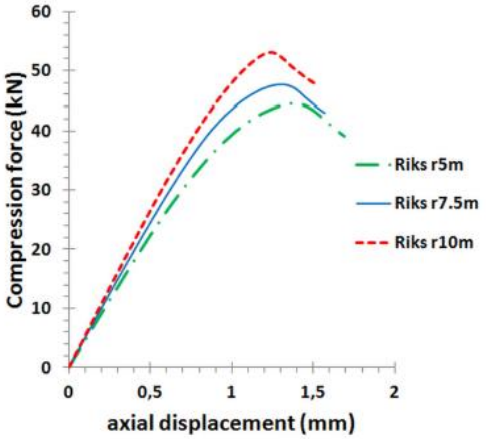

Fig. 13 Corrugated panel (Riks Method): load paths for different arch radiuses

It can be observed that for a straight panel, buckling and collapse modes represent well-known plate buckling phenomenon, which can consist of sine half-waves, where if web deforms towards inside, then flanges deform towards outside. For corrugated panels, local buckling is completely different. Deformation and failure was obtained in the form of the squeeze of corrugations (accordion behaviour) and it is presented in Fig. 14.

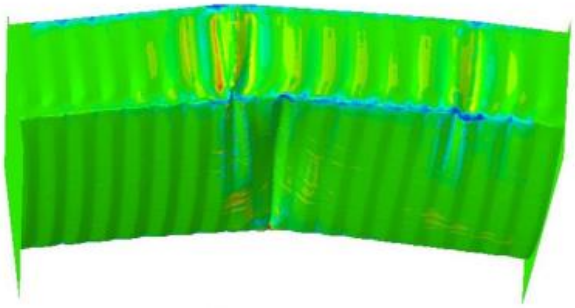

Fig. 14 Corrugated panel- accordion behavior

4. EXPERIMENTAL INVESTIGATION

4.1. Straight panel

Compression tests have been performed on straight panel samples with dimensions and the test setup presented in Fig 15. The displacement sensors were measuring the samples shortening from base equal around 200 mm as average value from six sensors (three outside and three inside of each sample). Displacement sensors were connected to a computer and they were independent of the hydraulic press. Force sensor was also connected to the computer but it was dependent on the hydraulic press. Hydraulic press was controlled by displacements (2 mm = 1 min). Load was applied at that cross-section gravity centre. It is impossible to compare experimental load displacement paths with numerical ones at this stage of research due to the following reasons: displacement sensors were independent of hydraulic press (this is the main reason caused by the lack of availability of the modern laboratory equipment); during experimental compression tests, when buckling occurred at the form of sine half-wave, displacement sensors lost their parallelism to the panel's axis (this was not a problem during corrugated panels compression tests due to accordion behaviour); during experimental tests, location of the load was constant (at the cross-section gravity, while during numerical investigation such location was changed (firstly load was applied at the gravity centre and then load was moved to the effective gravity centre).

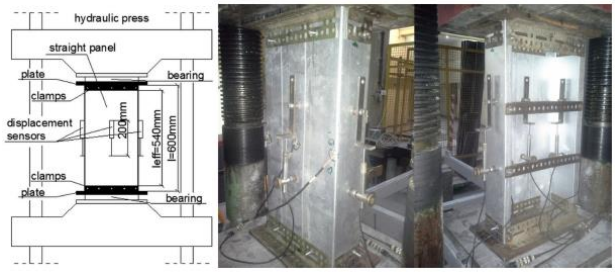

Fig. 15 Straight panel: test setup

In Fig. 16 obtained load-displacement paths are presented and it can be stated that all three tests were conducted with similar accuracy.

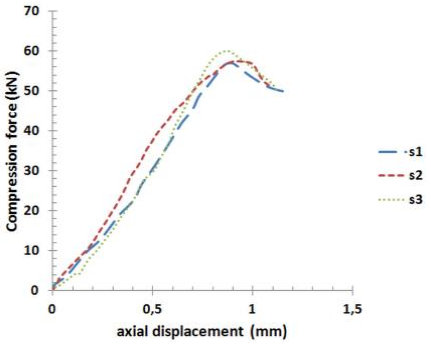

Fig. 16 Straight panel: test load paths

The ratio experimental failure load to numerical failure load is in range from 0.84 to 0.90 for numerical model which considers different material properties in corners areas. For numerical models with constant material properties such ratio is within the range 0.88-0.94. The small difference can be explained with unpredictable imperfections of the experiment. Fig. 17 shows deformed samples from experiential tests, and Fig. 18 form numerical analyses.

Fig. 17 Straight panel: experimental deformation shapes

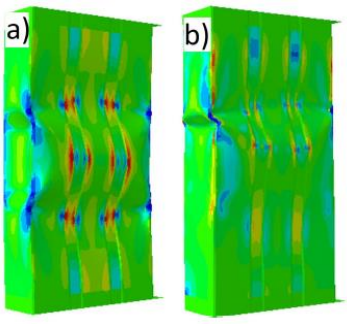

Fig. 18 Straight panel numerical deformation shapes

It can be observed that deformations from numerical analyses have similar form to the one from the compression test.

4.2. Doubly corrugated panel

Three samples for each arch radius (5 m,7.5 m, 10 m) were investigated. Fig. 19 shows test setup used for corrugated panels. Load (hydraulic pressure) was applied at the point of equivalent gravity centre.

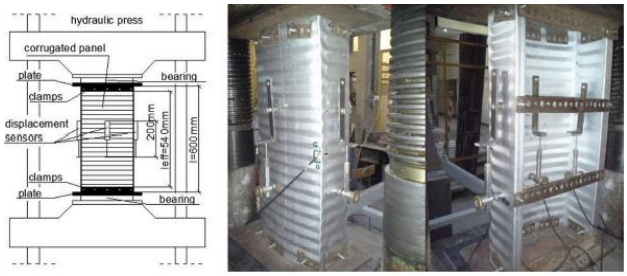

Fig. 19 Corrugated panel: test setup

In Figs 20, 21, 22 obtained load-displacement paths for each arch radius are presented and it can be stated that all three were conducted with similar accuracy.

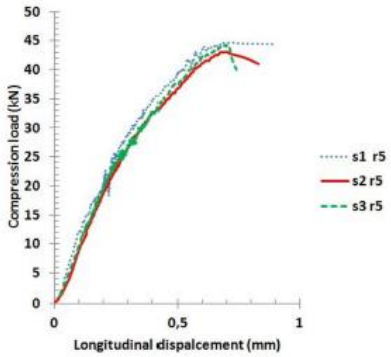

Fig. 20 Corrugated panel: test load paths, radius 5m

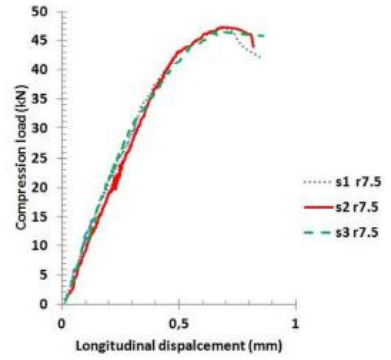

Fig. 21 Corrugated panel: test load paths, radius 7.5m

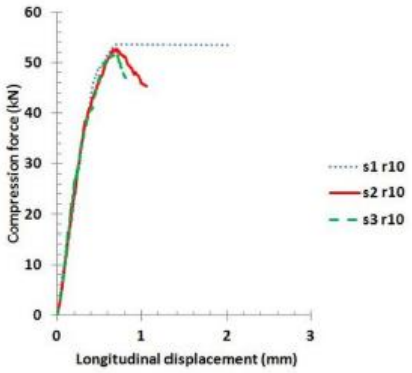

Fig. 22 Corrugated panel: test load paths, radius 10m

The ratio experimental failure load to numerical failure load is in range from 0.91 to 1.00 (Figs 23, 24, 25). Such good correlation is due to scanned geometry. So each compression test was designed based on very accurate FEM analyses. Experimental compression tests were conducted only to prove that chosen types of numerical analyses are appropriate.

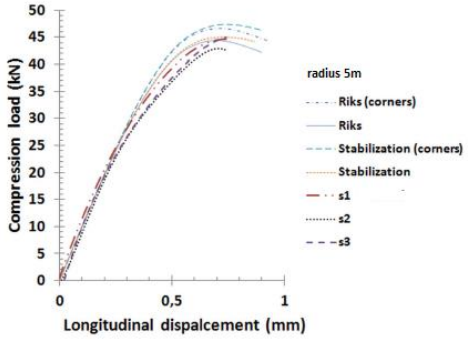

Fig. 23 Corrugated panel r5m: test and numerical load paths

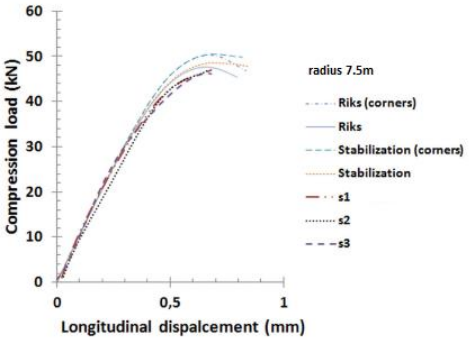

Fig. 24 Corrugated panel r7.5m: test and numerical load paths

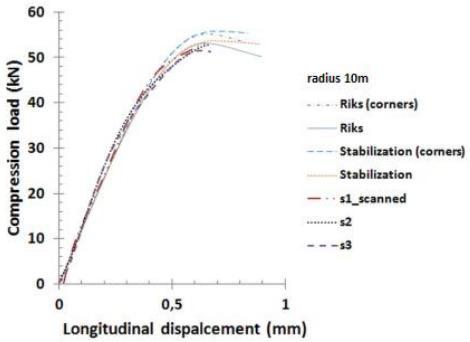

Fig. 25 Corrugated panel r10m: test and numerical load paths

Figs 26, 27, 28 compare examples of deformation shapes obtained from numerical and experimental investigations. It was observed that squeeze of single corrugations took place in the same locations. This also proves that numerical and experimental investigations have very good accuracy.

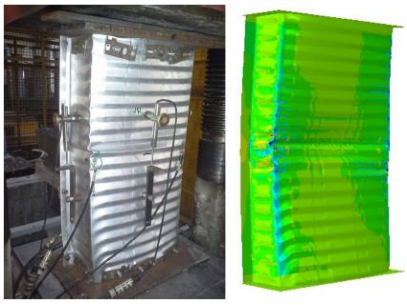
Fig. 26 Failures from numerical and experimental investigation (r5m)

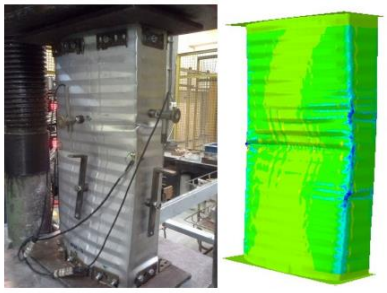
Fig. 27 Failures from numerical and experimental investigation (r7.5m)

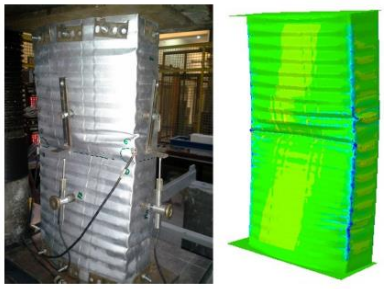
Fig. 28 Failures from numerical and experimental investigation (r10m)

5. CONCLUSIONS

It was observed that for straight panels (with smooth walls) linear stability analysis ends up with local buckling mode due to the bifurcation point. A value of critical compression force at this point lies on the elastic part of equilibrium path. Such behavior of a straight panel corresponds to the Class 4 cross-section described in Eurocode 3 Part 1-1 Ref. 2 and Eurocode 3 Part 1-5 Ref. 3 where general design rules for steel structures and plated structural elements are presented. Obtained values of ultimate loads from numerical analyses and compression tests were similar to the one obtained from Eurocode calculations. So it can be concluded that Eurocode 3 provides a very good procedure for an effective area calculation for local plate buckling investigation under axial compression load for thin-walled elements. It was also proved by laboratory compression tests.

Failure forces obtained from numerical analyses and laboratory tests have good accuracy results.

Local buckling will occur in Class 4 cross-sections before attainment of yield stress in the element. Such statement is not valid for curved panels where large surfaces imperfections called corrugations are machine pressed perpendicular to the panel longitudinal axis. Curved panel, according to the obtained results, losses its local stability due to the attainment of maximum load. There is no sign of instability on the elastic part of equilibrium path. In such case, curved panels cannot be treated as Class 4 cross-sections. It means that Eurocode 3 Part 1-5 Ref. 3 presents the calculations methods for thin-walled members where only longitudinal corrugations (along panel axis) are applicable. The values of ultimate loads or even failure loads from numerical analyses are much smaller than the value of ultimate load based on Eurocode 3 Part 1-5 Ref. 3. At this stage of research distortional buckling was neglected due to bracing applied during experimental investigation. The accuracy of numerical methods is proved by laboratory compression tests.

Generally speaking, this paper can be treated as a warning for engineers who often thoughtlessly use design standards. More detailed description of the research can be found in Refs 9, 10, 11, 12.

It is also important to write that research discussing ABM MIC 240 System is well presented in Refs 13, 14, 15, 16, 17.

REFERENCES

1. H.A. Mang, C.V. Girya Vallabhan, J.H. Smith: Finite element analysis of doubly corrugated shells. Journal of the Structural Division, 10 (12482):2033–2050, October 1976.
2. Eurocode 3- Part 1-1. Design of steel structures- Part 1-1: General rules and rules for buildings, EN 1993-1-1, 2007.

3. Eurocode 3- Part 1-5. Design of steel structures- Part 1-5: Plated structural elements, EN 1993-1-5, 2006.
4. R. Walentyński, R. Cybulski, J. Knapek: Budowa modelu teoretycznego podwójnie giętych paneli cienkościennych typu ABM 120. Aparatura Badawcza i Dydaktyczna. Vol. 18, No. 1, 2013.
5. R.D. Cook, D.S. Malkus, M.E. Plesha, R.J. Witt: Concepts and applications of finite element analysis. John Wiley & Sons, Inc, 4 edition, 2002.
6. E. Riks: The application of Newton's method to the problem of elastic stability. Journal of Applied Mechanics, 39:1060–1065, 1972.
7. DS Simulia. Abaqus Analysis User's Manual, Volume II: Analysis, 7.1.1 Solving Nonlinear Problems, 2011.
8. R. Cybulski : Analysis of local stability of doubly corrugated thin walled structures. PhD Thesis. Faculty of Civil Engineering. The Silesian University of Science. Gliwice 2015.
9. R. Walentynski, R. Cybulski, R. Sanchez: Numerical stability analyses and preliminary experimental investigation of doubly corrugated steel arch panels. Journal of IASS, Vol. 54, No.1, 2013.
10. R. Walentynski, M. Cybulska, R .Cybulski: Influence of geometric imperfections on the local stability of thin-walled elements. Shell Structures: Theory and Applications. Publisher: CRC Press, Taylor and Francis Group. Vol. 3, 9/2013.
11. R. Walentynski, R .Cybulski, K. Kozieł: Local buckling and post-buckling investigation of cold-formed self-supported elements. Recent Advances in Computational Mechanics, Mechanics of structures. Publisher: CRC Press, Taylor and Francis Group. Vol.20, 02/2014.
12. R. Cybulski, R. Walentynski, M. Cybulska: Local buckling of cold formed elements used in arched building with geometrical imperfections. Journal of Constructional Steel Research, 96, p. 1-13, 2014
13. A. Piekarczuk: Nowoczesne Rozwiązania Konstrukcyjne Hal Łukowych Dla Budownictwa Rolniczego. Budownictwo i Architektura, Vol. 12, n:259–66, 2013.
14. A. Piekarczuk: Podwójnie Gięte Samonośne Panele Dachowe. Materiały budowlane, 1 (6), p. 20–23, 2018.
15. A. Piekarczuk, M. Malesa, M. Kujawinska, K. Malowany: Application of Hybrid FEM-DIC Method for Assessment of Low Cost Building Structures. Experimental Mechanics, 52, p. 1297–1311, 2012.
16. A. Piekarczuk, K. Malowany: Comparative analysis of numerical models of arch-shaped steel sheet sections. Archives of civil and mechanical engineering, 16, p. 645–658, 2016.
17. A. Piekarczuk, P. Więch, K. Malowany: Numerical investigation into plastic hinge formation in arched corrugated thin-walled profiles. Thin-Walled Structures, 119, p. 13–21, 2017.